

# Twisted Electromagnetic Modes and Sagnac Ring-Lasers

David A. Burton\*  
 Adam Noble †  
 Robin W. Tucker‡  
 David L. Wiltshire§

September 20, 2018

## Abstract

A new approximation scheme, designed to solve the covariant Maxwell equations inside a rotating hollow slender conducting cavity (modelling a ring-laser), is constructed. It is shown that for well-defined conditions there exist TE and TM modes with respect to the longitudinal axis of the cavity. A twisted mode spectrum is found to depend on the integrated Frenet torsion of the cavity and this in turn may affect the Sagnac beat frequency induced by a non-zero rotation of the cavity. The analysis is motivated by attempts to use ring-lasers to measure terrestrial gravito-magnetism or the Lense-Thirring effect produced by the rotation of the Earth.

## 1 Introduction

In 1893 and 1897 Lodge argued that a device using electromagnetic fields should in principle be able to detect angular acceleration by the interference of light. Sixteen years later Sagnac [1] observed such an effect and realised the potential for light interferometers as accelerometers. The continued development of such instruments and their careful exploitation by Michelson and others was pivotal in the establishment of our current world view of classical physics. Sagnac recognised that his observations could open up new avenues in the development of accelerometers, an insight that has been dramatically verified. Today the ring-laser is a cornerstone of most inertial

---

\*Department of Physics, Lancaster University, UK (email : d.burton@lancaster.ac.uk)

†Department of Physics, Lancaster University, UK (email : a.noble1@lancaster.ac.uk)

‡Department of Physics, Lancaster University, UK (email : r.tucker@lancaster.ac.uk)

§Department of Physics and Astronomy, University of Canterbury, Private Bag 4800, Christchurch, NZ (email : david.wiltshire@canterbury.ac.nz)

guidance systems and optoelectronics is the backbone of the communications industry (see [2, 3, 4] for historical accounts of ring-laser development).

The basic principles leading to the Sagnac effect are well understood in broad outline. As with all interferometers, a guided wave phenomenon (such as that experienced by electromagnetic fields in a wave guide) is used to distinguish different propagation paths in spacetime. The traditional electromagnetic “passive” type of Sagnac interferometer involves splitting a light beam into two coherent components, forcing them to travel different paths in spacetime to an event where they combine to produce an interference pattern. The nature of the interference fringes can then be correlated with the difference in the optical paths. In such a device the frequency of the light employed is controlled externally and the circuits in spacetime are often determined by mirrors or continuous dielectric fibres.

With the discovery of the laser it was found that the electromagnetic modes of a closed tubular cavity containing an active lasing medium (excited initially by an external RF field) could be made to produce an interference pattern that varied with the state of rotation of the whole apparatus. Such an instrument has been labelled an “active” device to distinguish it from the traditional passive Sagnac interferometer. Certain modes of a non-rotating cavity can be made to form standing waves. However, the co- and counter-propagating modes in a rotating lasing cavity acquire different resonant frequencies leading to a beat-frequency as observed by an on-board probe. In 1963 Sperry-Rand recognised that the active ring-laser could be used as an inertial-guidance device. Today such miniturised interferometers are used routinely in civil and military applications.

Considerable increase in sensitivity can be achieved using larger ring-lasers. Insulated from thermal and seismic noise, sensitivities of  $10^{-8}$  are routinely obtained in the UG1 Sagnac interferometer housed in the Cashmere Cavern in Christchurch, New Zealand. With an effective area of  $367.6\text{m}^2$  and perimeter 77m it operates with a He-Ne laser at 474THz and an intracavity power of 50mW at each mirror. High resolution can be achieved by pattern matching to periodic variation of the Sagnac frequency induced by rotation of the Earth. Using matching based on geophysical modelling, detection of lunar perturbations of the Earth’s rotation and the amplitudes of the Oppolzer modes have recently been reported in [6]. The instantaneous direction of the Earth’s rotation axis has been measured to a precision of 1 part in  $10^8$  when averaged over a time interval of several hours.

The enhanced sensitivity of such large ring-lasers owes much to the significant improvement of mirror design in recent years. It is imperative for the maintenance of a Sagnac beat signal that pollution of the resonant state by competing modes is inhibited. This requires considerable engineering skill, the use of thermally inert materials and mirrors that can maintain the dominant cavity resonant mode over long periods of time.

With such advances in technology it is natural to seek the sensitivities that are necessary to discriminate the effects of non-Newtonian gravitation on the behaviour of light [5]. The most important of these is the gravito-magnetic field of the rotating Earth, predicted by Einstein's description of gravitation.

However, even crude estimates of the effects of terrestrial gravito-magnetism show that a number of competing effects that may modify the classical Sagnac effect (due to the rotation of the apparatus) need careful consideration. Such effects are often dependent on the structure of the interferometer and so invite one to contemplate alternative designs. Although, in general, one expects that the sensitivity of an active ring-laser will increase with its spatial dimensions one may also enquire about the dependence of sensitivity on its geometry and spatial shape. In order to discriminate gravito-magnetic effects it then becomes necessary to understand in some detail how the geometry and shape of the interferometer affect the resonant mode structure of the cavity. In this way one can hope to discriminate between a number of features that compete to modify the classical Sagnac frequency.

The effect of gravitation on the Sagnac beat frequency is usually discussed in terms of the high frequency ray-optic description of light. In this way one can simply relate the interference of co- and counter-propagating electromagnetic modes to the proper time difference between events that terminate their ray histories in spacetime [7]. While such an analysis can give valuable insights into the leading terms in an asymptotic expansion in the lasing frequency it cannot address the effects due to the vector nature of the electromagnetic modes and the effects of the infinity of competing modes possessed by the lasing cavity.

An exact analysis of the wave nature of light in an active Sagnac cavity is a non-trivial mathematical problem that has to our knowledge never been fully considered. The problem is complicated by the fact that the harmonic electromagnetic modes rarely split into simpler transverse electric (TE) and transverse magnetic (TM) modes that greatly simplify the analysis in most simply-connected axially symmetric cavity geometries. Such a separation relies on a number of factors such as the shape of the entire cavity in space, the homogeneity of the lasing medium, the nature of the acceleration of the cavity and the presence of even a weak non-Newtonian gravitational field.

In order to accommodate these complexities a viable approximation is mandatory. Here the problem is approached in terms of an expansion scheme determined by scales related to the geometry of the cavity. Thus slender cavities are considered where the ratio of the transverse dimension to the cavity length is small. Such cavities will be called "wavetubes". In order to confidently predict near-Earth general relativistic contributions to the active Sagnac beat frequency a careful electromagnetic mode analysis of the cavity must be considered. This can be done in terms of the covariant Maxwell equations [8, 9] for moving media [13] on a background spacetime deter-

mined by Einstein's equations for gravitation. The procedure will exploit a local system of coordinates adapted to the geometry of a wavetube. Such a wavetube can be characterised in terms of the locus in space of the centre of each of its transverse cross-sections. This locus is regarded as a closed space curve with possible non-zero Frenet torsion and curvature. The approximation scheme will be developed for a wavetube with central locus having local curvature departing slightly from that of a fixed plane circle.

In sections 2 and 3 it is shown how to construct TE and TM type solutions to the covariant Maxwell equations for a particular class of coframes. These include the fields in rotating cavities containing a homogenous, isotropic and dispersionless medium in the presence of terrestrial gravito-magnetism. The language of exterior differential forms is used throughout since it offers the most succinct formulation for the field equations and makes clear the role of the spacetime metric and local coframe that feature in the subsequent computational scheme. The relation to the inertial 3-d formulation can be found in [14] and references therein. In section 4 a particular coordinate system is introduced that, together with a particular Frenet frame, encodes the geometry of the wavetube and permits one to introduce dimensionless parameters that control the nature of the approximation scheme. In these coordinates differences between non-inertial motion and gravito-magnetic effects are made explicit in sections 5.1 and 5.2. A complete mode analysis of the rotating wavetube is given in section 6 and the effects of multi-mode excitation and the description of Sagnac beats is explored in section 7. In particular attention is drawn to the effects of non-planarity of the wavetube on the beat frequency by reference to a particular geometry generated by the structure of a torus-knot.

## 2 Exact solutions to the vacuum Maxwell equations

To accommodate the ideas above it is first shown how a class of spacetime metrics that admit local orthonormal coframes with particular properties are sufficient to construct TE and TM type electromagnetic modes relative to such a coframe. The language of exterior forms is used throughout<sup>1</sup> since this greatly facilitates the discussion and leads in a direct manner to an explicit construction of the fields below. The hollow wavetube is supposed to be constructed of a perfectly conducting material which in this section contains no lasing medium.

Let  $(\mathcal{M}, g)$  be a spacetime and let  $\{e^0, e^1, e^2, e^3\}$  be a local orthonormal

---

<sup>1</sup>Lowercase indices at the beginning of the Latin alphabet  $\{a, b, c, \dots\}$  range over the integers  $\{0, 1, 2, 3\}$ , indices in the middle of the Latin alphabet  $\{j, k, l, \dots\}$  range over the integers  $\{2, 3\}$  and Greek indices  $\{\alpha, \beta, \gamma, \dots\}$  range over  $\{0, 1\}$ . Expressions involving repeated indices imply use of the Einstein summation convention.

coframe with respect to the metric tensor

$$g = -e^0 \otimes e^0 + e^1 \otimes e^1 + e^2 \otimes e^2 + e^3 \otimes e^3$$

with dual frame  $\{X_0, X_1, X_2, X_3\}$ ,

$$e^a(X_b) = \delta_b^a, \tag{1}$$

and orientation (volume form) defined by the Hodge map  $\star$  with

$$\star 1 = e^0 \wedge e^1 \wedge e^2 \wedge e^3.$$

The inverse metric tensor  $g^{-1}$  is

$$g^{-1} = -X_0 \otimes X_0 + X_1 \otimes X_1 + X_2 \otimes X_2 + X_3 \otimes X_3.$$

Define the split of the cotangent space  $T_p^*\mathcal{M} = (T_p^*\mathcal{M})^\parallel \oplus (T_p^*\mathcal{M})^\perp$  with  $(T_p^*\mathcal{M})^\parallel$  spanned by  $\{e^0, e^1\}$  and  $(T_p^*\mathcal{M})^\perp$  spanned by  $\{e^2, e^3\}$  at  $p \in \mathcal{M}$ . These subspaces inherit Hodge maps with  $\#1 = e^0 \wedge e^1$  and  $\#\perp 1 = e^2 \wedge e^3$  so

$$\star 1 = \#1 \wedge \#\perp 1.$$

Now restrict to spacetime metrics  $g$  that admit local orthonormal coframes satisfying the conditions

$$\begin{aligned} de^\alpha &= 0, \\ d\#\perp 1 &= 0. \end{aligned} \tag{2}$$

These conditions permit a viable approximation scheme leading to a tractable decomposition of electromagnetic modes in a wide context to be discussed below.

A differential form  $\mu$  (vector field  $X$ ) on  $\mathcal{M}$  that satisfies  $\iota_{X_j}\mu = 0$  ( $e^j(X) = 0$ ) for all  $j$  will be called *longitudinal*<sup>2</sup>. A *transverse* differential form  $\nu$  (vector field  $Y$ ) will satisfy  $\iota_{X_\alpha}\nu = 0$  ( $e^\alpha(Y) = 0$ ) for all  $\alpha$ .

Let the 2-form  $F$  be a solution to the vacuum Maxwell equations

$$\begin{aligned} dF &= 0, \\ d\star F &= 0 \end{aligned} \tag{3}$$

in a spacetime region bounded by a perfectly conducting wavetube hypersurface  $\mathcal{B} \equiv \{p \in \mathcal{M} : f(p) = 0, df \text{ timelike}\}$  and subject to the boundary condition

$$(df \wedge F)(p) = 0 \quad \forall p \in \mathcal{B}. \tag{4}$$

---

<sup>2</sup> $\iota_X$  is the interior derivative on forms with respect to the vector field  $X$ .

The wavetube interior on spacetime is topologically  $\mathbf{R} \times S^1 \times \mathbf{D}$  where  $\mathbf{D}$  is a 2-disc. Solutions to Maxwell's equations are sought by adapting the above coframe to the wavetube geometry. Furthermore, we shall suppose that (4) must be satisfied with  $df(p)$ , for all  $p \in \mathcal{B}$ , a transverse 1-form. Since  $de^\alpha = 0$  the pair  $\{e^0, e^1\}$  are, by Frobenius' theorem, normal 1-forms to a local foliation  $\mathcal{F}$  of  $\mathcal{M}$ . The leaves of  $\mathcal{F}$  contain the wavetube cross-sections, each of whose intersection with  $\mathcal{B}$  is the image of a closed curve.

Locally, we seek separable propagating solutions of the form  $F = \exp(iW)\gamma$  for some 2-form  $\gamma$  where

$$dW = \xi_\alpha e^\alpha \equiv \xi \neq 0$$

for constant components  $\{\xi_0, \xi_1\}$ . We decompose  $\gamma$  into longitudinal and transverse parts

$$\begin{aligned} \gamma &= \Phi \# 1 + \Psi \#_{\perp} 1 + e^\alpha \wedge \Theta_\alpha, \\ \Theta_\alpha(X_\beta) &= 0, \\ d\Phi(X_\alpha) &= 0, \\ d\Psi(X_\alpha) &= 0, \\ \iota_{X_\alpha} d\Theta_\beta &= 0. \end{aligned}$$

Thus  $\{d\Phi, d\Psi, \Theta_0, \Theta_1\}$  are transverse 1-forms and  $\{d\Theta_0, d\Theta_1\}$  are transverse 2-forms. Using the identity

$$\star(\alpha \wedge \tilde{X}) = \iota_X \star \alpha,$$

where  $\tilde{X} \equiv g(X, -)$  for any vector field  $X$  on  $\mathcal{M}$  and  $\alpha$  is any  $p$ -form on  $\mathcal{M}$  it can be shown that

$$\star(\mu \wedge \nu) = (-1)^{(2-p)q} \# \mu \wedge \#_{\perp} \nu \quad (5)$$

where  $\mu$  is a longitudinal  $p$ -form,  $\nu$  is a transverse  $q$ -form and

$$\begin{aligned} \#(\alpha \wedge \tilde{X}) &= \iota_X \# \alpha, \\ \#_{\perp}(\alpha \wedge \tilde{X}) &= \iota_X \#_{\perp} \alpha. \end{aligned}$$

Inserting the expression for  $F$  into Maxwell's equations (3) gives

$$\begin{aligned} d\Phi \wedge \# 1 - e^\alpha \wedge d\Theta_\alpha + i\xi \wedge (\Psi \#_{\perp} 1 + e^\alpha \wedge \Theta_\alpha) &= 0, \\ d\Psi \wedge \# 1 + \# e^\alpha \wedge d\#_{\perp} \Theta_\alpha - i\xi \wedge (\Phi \#_{\perp} 1 + \# e^\alpha \wedge \#_{\perp} \Theta_\alpha) &= 0 \end{aligned}$$

where (5) has been used. The form structure indicates that the above pair splits into

$$d\Phi \wedge \# 1 + i\xi \wedge e^\alpha \wedge \Theta_\alpha = 0, \quad (6)$$

$$e^\alpha \wedge d\Theta_\alpha - i\xi \wedge \Psi \#_{\perp} 1 = 0, \quad (7)$$

$$d\Psi \wedge \# 1 - i\xi \wedge \# e^\alpha \wedge \#_{\perp} \Theta_\alpha = 0, \quad (8)$$

$$\# e^\alpha \wedge d\#_{\perp} \Theta_\alpha - i\xi \wedge \Phi \#_{\perp} 1 = 0. \quad (9)$$

Acting with  $\star$  on (6) and (8) and using (5) yields

$$\Theta_{(\#\xi)} = -id\Phi, \quad (10)$$

$$\Theta_{(\xi)} = i\#_{\perp}d\Psi \quad (11)$$

where  $\Theta_{(\xi)} = \xi^{\alpha}\Theta_{\alpha}$  and  $\Theta_{(\#\xi)} = (\#\xi)^{\alpha}\Theta_{\alpha}$ . Acting with  $\iota_{\tilde{\xi}}$ , where  $\tilde{\xi} = g^{-1}(\xi, -)$ , on equation (7) yields

$$d\Theta_{(\xi)} = i\xi^2\Psi\#_{\perp}1 \quad (12)$$

where  $\xi^2 \equiv g^{-1}(\xi, \xi)$ . Similarly, (9) leads to

$$d\#_{\perp}\Theta_{(\#\xi)} = -i\xi^2\Phi\#_{\perp}1. \quad (13)$$

Thus, inserting (10) in (13) and (11) in (12) yields

$$d\#_{\perp}d\Phi = \xi^2\Phi\#_{\perp}1, \quad (14)$$

$$d\#_{\perp}d\Psi = \xi^2\Psi\#_{\perp}1. \quad (15)$$

The Helmholtz equations (14) and (15) determine  $\Phi$  and  $\Psi$  subject to (4). The boundary condition (4) may be expanded

$$df(p) \wedge (\Phi\#1 + e^{\alpha} \wedge \Theta_{\alpha})(p) = 0 \quad \forall p \in \mathcal{B}$$

implying

$$\Phi(p) = 0 \quad \forall p \in \mathcal{B}, \quad (16)$$

$$(df \wedge e^{\alpha} \wedge \Theta_{\alpha})(p) = 0 \quad \forall p \in \mathcal{B}. \quad (17)$$

In general there are three possibilities for the metric norm  $\xi^2 = g^{-1}(\xi, \xi)$  of  $\xi$  :

- $\xi^2 = 0$ .

#### Triviality of $\Phi$

Let  $S$  be a 2-chain for which the image of  $\partial S$  is in  $\mathcal{B}$  and  $(\partial S)^*df = 0$  and note

$$\begin{aligned} \int_S d\bar{\Phi} \wedge \#_{\perp}d\Phi &= \int_{\partial S} \bar{\Phi}\#_{\perp}d\Phi - \int_S \bar{\Phi}d\#_{\perp}d\Phi \\ &= -\xi^2 \int_S |\Phi|^2\#_{\perp}1 \end{aligned} \quad (18)$$

using (14) and (16) where  $\bar{\Phi}$  is the complex-conjugate of  $\Phi$ . Since

$$\#_{\perp}^{-1}(\beta \wedge \#_{\perp}\beta) \geq 0 \quad (19)$$

where  $\beta$  is any transverse  $p$ -form and, by hypothesis,  $\xi^2 = 0$  it follows from (18) that  $d\Phi = 0$  and so, using (16),  $\Phi = 0$ .

### Triviality of $\Psi$ and $F$

Since  $\xi$  is null  $\#\xi$  is proportional to  $\xi$  and so (10) and (11) with  $\Phi = 0$  imply that  $\Theta_{(\xi)}$  vanishes and  $\Psi$  is constant. Let  $\zeta = \zeta_\alpha e^\alpha$  be the null longitudinal 1-form with constant components  $\zeta_\alpha$  that satisfies  $g^{-1}(\xi, \zeta) = 1$ . Acting with  $\iota_{\tilde{\zeta}}$  on (9) and (7) and noting  $\#\zeta = \varepsilon\zeta$  where  $|\varepsilon| = 1$  it is found that

$$d\#\perp\Theta_{(\zeta)} = 0, \quad (20)$$

$$d\Theta_{(\zeta)} = i\Psi\#\perp 1. \quad (21)$$

Since  $\Theta_{(\xi)}$  vanishes  $e^\alpha \wedge \Theta_\alpha = (\xi^\alpha \zeta + \zeta^\alpha \xi) \wedge \Theta_\alpha = \xi \wedge \Theta_{(\zeta)}$  where  $\xi^\alpha = g^{-1}(e^\alpha, \xi)$  and  $\zeta^\alpha = g^{-1}(e^\alpha, \zeta)$ . The differential form  $df \wedge \Theta_{(\zeta)}$  is transverse and so

$$(df \wedge \Theta_{(\zeta)})(p) = 0 \quad \forall p \in \mathcal{B} \quad (22)$$

follows from (17). By integrating (21) over the 2-chain  $S$  introduced earlier, noting that (22) implies  $(\partial S)^*\Theta_{(\zeta)} = 0$  and recalling that  $\Psi$  is constant, it follows that  $\Psi = 0$  and

$$d\Theta_{(\zeta)} = 0.$$

Cross-sections of the wavetube interior are simply-connected and so by the Poincaré lemma [17]

$$\Theta_{(\zeta)} = d\varphi. \quad (23)$$

It follows from (20) and (22) that  $\varphi$  satisfies

$$d\#\perp d\varphi = 0 \quad (24)$$

subject to the Dirichlet boundary condition

$$\varphi(p) = \varphi_0 \quad \forall p \in \mathcal{B} \quad (25)$$

where  $\varphi_0$  is a complex constant. The solution to (24) and (25) is  $\varphi = \varphi_0$  and so, using (23),  $\Theta_{(\zeta)} = 0$  and

$$F = 0.$$

- $\xi^2 > 0$ .

### Triviality of $\Phi$

Using (18) and (19) it can be seen that  $\Phi$  vanishes since, by hypothesis,  $\xi^2 > 0$ .



### Triviality of $\Psi$ and $F$

Introduce the spacelike normalized 1-form  $m = \xi/\sqrt{\xi^2}$  and write

$$\begin{aligned}\Theta_\alpha &= m_\alpha \Theta_{(m)} - (\#m)_\alpha \Theta_{(\#m)} \\ &= m_\alpha \Theta_{(m)}\end{aligned}$$

where  $m_\alpha = m(X_\alpha)$  and  $(\#m)_\alpha = (\#m)(X_\alpha)$  and  $\Theta_{(\#m)}$  vanishes by (10) because  $\Phi = 0$ . Thus (17) yields

$$(df \wedge \xi \wedge \Theta_{(\xi)})(p) = 0 \quad \forall p \in \mathcal{B}.$$

Since  $\xi$  is longitudinal and  $df \wedge \#_\perp d\Psi$  is transverse (11) gives the Neumann boundary condition

$$(df \wedge \#_\perp d\Psi)(p) = 0 \quad \forall p \in \mathcal{B}. \quad (26)$$

The simple-connectedness of the wavelube cross-sections implies that the eigenvalues  $\xi^2$  in (15) associated with the Neumann boundary condition (26) are negative. To prove this an argument similar to that used in the Dirichlet case is employed. Let  $S$  be the 2-chain introduced earlier and note that (26) implies  $\#_\perp d\Psi = hdf$ , where  $h$  is a 0-form, and

$$(\partial S)^*(\#_\perp d\Psi) = 0 \quad (27)$$

since  $(\partial S)^*df = 0$ . Thus

$$\begin{aligned}\int_S d\bar{\Psi} \wedge \#_\perp d\Psi &= \int_{\partial S} \bar{\Psi} \#_\perp d\Psi - \int_S \bar{\Psi} d\#_\perp d\Psi \\ &= -\xi^2 \int_S |\Psi|^2 \#_\perp 1\end{aligned} \quad (28)$$

using (15) and (27) where  $\bar{\Psi}$  is the complex-conjugate of  $\Psi$ . By hypothesis  $\xi^2 > 0$  and using (19) it follows that  $\Psi = 0$ . Therefore

$$F = 0.$$

- $\xi^2 < 0$ .

This is the only situation that leads to a non-trivial expression for  $F$ . Introduce the timelike normalized 1-form  $m = \xi/|\xi|$  and write

$$\begin{aligned}\Theta_\alpha &= -m_\alpha \Theta_{(m)} + (\#m)_\alpha \Theta_{(\#m)} \\ &= -i\#_\perp d\Psi \frac{\xi_\alpha}{|\xi|^2} - id\Phi \frac{(\#\xi)_\alpha}{|\xi|^2}\end{aligned}$$

where  $|\xi| \equiv \sqrt{-\xi^2}$  and (10) and (11) have been used. Inserting the above equation for  $\Theta_\alpha$  into the boundary condition (17) yields

$$\left[ df \wedge \left( \frac{\xi}{|\xi|^2} \wedge \#_\perp d\Psi + \frac{\#_\perp \xi}{|\xi|^2} \wedge d\Phi \right) \right] (p) = 0 \quad \forall p \in \mathcal{B}.$$

However, (16) means that  $d\Phi$  on  $\mathcal{B}$  is proportional to  $df$  and so again (26) is obtained.

Expressed entirely in terms of  $\{\Phi, \Psi, W\}$  the Maxwell 2-form  $F$  can be written  $F = F_{TM} + F_{TE}$  where

$$F_{TM} = \left[ \Phi \#_\perp 1 - i \frac{\#_\perp dW_{TM}}{|dW_{TM}|^2} \wedge d\Phi \right] \exp(iW_{TM}), \quad (29)$$

$$F_{TE} = \left[ \Psi \#_\perp 1 - i \frac{dW_{TE}}{|dW_{TE}|^2} \wedge \#_\perp d\Psi \right] \exp(iW_{TE}). \quad (30)$$

The Helmholtz equations for  $\Phi$  and  $\Psi$  are

$$\begin{aligned} d\#_\perp d\Phi &= -|dW_{TM}|^2 \Phi \#_\perp 1, \\ d\#_\perp d\Psi &= -|dW_{TE}|^2 \Psi \#_\perp 1 \end{aligned}$$

solved subject to the boundary conditions

$$\begin{aligned} \Phi(p) &= 0 \quad \forall p \in \mathcal{B}, \\ (df \wedge \#_\perp d\Psi)(p) &= 0 \quad \forall p \in \mathcal{B} \end{aligned}$$

where  $dW_{TM} = \xi_\alpha^{TM} e^\alpha$  and  $dW_{TE} = \xi_\alpha^{TE} e^\alpha$  are timelike. The constants  $\{\xi_\alpha^{TM}, \xi_\alpha^{TE}\}$  are determined by the appropriate boundary conditions and, in general,  $dW_{TE} \neq dW_{TM}$ .

### 3 Exact solutions to the Maxwell equations in a medium

To excite electromagnetic modes in a wavetube one may fill it with a gas such as a helium-neon mixture and induce it to lase with an external RF field. The presence of a lasing medium requires that one take into account its electrical and magnetic susceptibility. The electromagnetic field in a material medium is described by a pair of 2-forms  $\{F, G\}$  on spacetime that satisfy the equations:

$$\begin{aligned} dF &= 0, \\ d \star G &= j \end{aligned}$$

where  $j$  is a source 3-form.

For a given  $j$ , the 2-form  $G$  must be related to  $F$  in order to have a closed system. This is usually done by relating their components relative to decompositions of the form:

$$\begin{aligned} F &= E \wedge \tilde{V} + B, \\ G &= D \wedge \tilde{V} + H \end{aligned}$$

where the timelike vector  $V$  is normalised with  $g(V, V) = -1$  and the forms  $\{E, B, D, H\}$  are all annihilated by  $\iota_V$ . With a spacetime metric tensor  $g$ , having physical dimensions of length squared, a coherent dimensional scheme arises with the aid of the permittivity constant  $\epsilon_0$  and permeability  $\mu_0$  of free space satisfying  $\epsilon_0 \mu_0 = \frac{1}{c^2}$  where  $c$  is the speed of light in vacuum. In terms of conventional MKS components of electric and magnetic fields one has in any  $g$ -orthonormal coframe  $\{f^0 = -\tilde{V}, f^1, f^2, f^3\}$  adapted to  $V$ :

$$\begin{aligned} E &:= \epsilon_0 E^{MKS} = \epsilon_0 (E_1^{MKS} f^1 + E_2^{MKS} f^2 + E_3^{MKS} f^3), \\ B &:= \frac{1}{\mu_0} B^{MKS} = \frac{1}{\mu_0} (B_1^{MKS} f^2 \wedge f^3 + B_2^{MKS} f^3 \wedge f^1 + B_3^{MKS} f^1 \wedge f^2). \end{aligned}$$

For  $G$  one has  $D = D^{MKS}$  and  $H = H^{MKS}$ . For a linear isotropic homogeneous dispersionless non-conducting medium with relative permittivity  $\epsilon_r$  and relative permeability  $\mu_r$  one has the simple constitutive relations  $D = \epsilon_r E$  and  $H = B/\mu_r$  or

$$G = \left(\epsilon_r - \frac{1}{\mu_r}\right) \iota_V F \wedge \tilde{V} + \frac{1}{\mu_r} F.$$

Such a constitutive relation assumes that the dimensionless quantities  $\epsilon_r$  and  $\mu_r$  are frame-independent constant scalars on spacetime. The refractive index  $\mathcal{N}$  of the medium is

$$\mathcal{N} = \sqrt{\epsilon_r \mu_r}.$$

Propagating solutions to the source-free Maxwell equations

$$\begin{aligned} dF &= 0, \\ d \star G &= 0 \end{aligned} \tag{31}$$

that satisfy the boundary condition

$$(df \wedge F)(p) = 0 \quad \forall p \in \mathcal{B}$$

at the wavetube surface  $\mathcal{B}$ ,

$$\mathcal{B} = \{p \in \mathcal{M} : f(p) = 0\}, df \text{ timelike,}$$

have a similar structure to (29) and (30) when  $V$  has the form

$$V = V^\alpha X_\alpha,$$

where  $\{V^\alpha\}$  are constant and  $\{X_\alpha\}$  belong to the frame  $\{X_a\}$  dual to the coframe  $\{e^a\}$  satisfying the conditions (2).

It can be shown that  $F_{TM}$  and  $F_{TE}$  are solutions to (31) where

$$F_{TM} = \left[ \Phi \# 1 - i \frac{\# \beta_{TM}}{|\alpha_{TM}|^2} \wedge d\Phi \right] \exp(iW_{TM}), \quad (32)$$

$$F_{TE} = \left[ \Psi \#_{\perp} 1 - i \frac{dW_{TE}}{|\alpha_{TE}|^2} \wedge \#_{\perp} d\Psi \right] \exp(iW_{TE}) \quad (33)$$

with

$$\begin{aligned} \alpha_{TM} &= (1 - \mathcal{N})dW_{TM}(V)\tilde{V} + dW_{TM}, \\ \alpha_{TE} &= (1 - \mathcal{N})dW_{TE}(V)\tilde{V} + dW_{TE}, \\ \beta_{TM} &= (1 - \mathcal{N}^2)dW_{TM}(V)\tilde{V} + dW_{TM}. \end{aligned} \quad (34)$$

The Helmholtz equations for  $\Phi$  and  $\Psi$  are

$$\begin{aligned} d\#_{\perp}d\Phi &= -|\alpha_{TM}|^2\Phi\#_{\perp}1, \\ d\#_{\perp}d\Psi &= -|\alpha_{TE}|^2\Psi\#_{\perp}1 \end{aligned}$$

and are solved subject to the boundary conditions

$$\begin{aligned} \Phi(p) &= 0 \quad \forall p \in \mathcal{B}, \\ (df \wedge \#_{\perp}d\Psi)(p) &= 0 \quad \forall p \in \mathcal{B}. \end{aligned}$$

As before  $dW_{TM} = \xi_{\alpha}^{TM}e^{\alpha}$  and  $dW_{TE} = \xi_{\alpha}^{TE}e^{\alpha}$  where  $\{\xi_{\alpha}^{TM}\}$  and  $\{\xi_{\alpha}^{TE}\}$  are constant.

## 4 Twisted ring cavities rotating in space

### 4.1 Moving space curves

A moving space curve in Euclidean  $\mathbf{R}^3$  may be represented by a  $\mathbf{R}^3$ -valued mapping  $(s, t) \mapsto \mathbf{C}(s, t)$ . Suppose that  $s$  parameterises arc length and  $t$  is a time variable. The instantaneous geometry of the space curve may be described by three mutually orthogonal unit vectors  $\{\mathbf{t}, \mathbf{n}, \mathbf{b}\}$  on the image of  $\mathbf{C}$  at each time  $t_0$ . For a Frenet frame with  $\mathbf{t}$  tangent to  $\mathbf{C}(s, t_0)$  one has:

$$\begin{aligned} \mathbf{C}' &= \mathbf{t}, \\ \mathbf{t}' &= \kappa\mathbf{n}, \\ \mathbf{n}' &= -\kappa\mathbf{t} + \tau\mathbf{b}, \\ \mathbf{b}' &= -\tau\mathbf{n} \end{aligned} \quad (35)$$

where  $f'$  denotes the derivative of  $f$  with respect to  $s$  and  $\kappa(s, t_0)$  and  $\tau(s, t_0)$  denote the curvature and torsion of  $\mathbf{C}(s, t_0)$  respectively. We shall restrict

our discussion to space curves that admit continuous Frenet frames along their entire length. Since the triad  $(\mathbf{t}, \mathbf{n}, \mathbf{b})$  forms an orthonormal basis on the curve the time derivative  $(\dot{\mathbf{t}}, \dot{\mathbf{n}}, \dot{\mathbf{b}})$  is related to  $(\mathbf{t}, \mathbf{n}, \mathbf{b})$  by an anti-symmetric matrix for each  $(s, t)$ . We are interested in space curves that rotate rigidly with uniform angular velocity  $\boldsymbol{\Omega}$  without deformation. Thus  $\boldsymbol{\Omega}' = 0, \dot{\boldsymbol{\Omega}} = 0, \dot{\kappa} = \dot{\tau} = 0$  and  $\dot{\mathbf{C}} = \boldsymbol{\Omega} \times \mathbf{C}$ .

These imply

$$\begin{aligned}\dot{\mathbf{t}} &= \boldsymbol{\Omega} \times \mathbf{t}, \\ \dot{\mathbf{n}} &= \boldsymbol{\Omega} \times \mathbf{n}, \\ \dot{\mathbf{b}} &= \boldsymbol{\Omega} \times \mathbf{b}.\end{aligned}\tag{36}$$

In a fixed global cartesian triad  $(\mathbf{i}, \mathbf{j}, \mathbf{k})$  one may write in cylindrical coordinates:

$$\mathbf{C} = C_r \cos(C_\theta) \mathbf{i} + C_r \sin(C_\theta) \mathbf{j} + C_k \mathbf{k}.$$

If this triad is oriented so that  $\boldsymbol{\Omega} = \Omega \mathbf{k}$  then  $C_k$  and  $C_r$  are independent of  $t$  and  $C_\theta(s, t) = C_\theta(s) + \Omega t$ .

Let the vector  $\mathbf{r}_{t_0}$  with Cartesian components  $(y_1, y_2, y_3)$  in the frame  $(\mathbf{i}, \mathbf{j}, \mathbf{k})$ ,

$$\mathbf{r}_{t_0} = y_1 \mathbf{i} + y_2 \mathbf{j} + y_3 \mathbf{k},$$

locate a point at the instant  $t_0$ . If this point lies in a tubular neighbourhood about the space curve  $\mathbf{C}(s, t_0)$  it may also be labelled by the Frenet coordinates  $(s, x_1, x_2)$  such that:

$$\mathbf{r}_{t_0} = \mathbf{C}(s, t_0) + x_1 \mathbf{n}(s, t_0) + x_2 \mathbf{b}(s, t_0)$$

Thus for points in this region one has a transformation between the Cartesian coordinates  $(y_1, y_2, y_3)$  and the Frenet coordinates  $(s, x_1, x_2)$ .

When the curve moves

$$d\mathbf{r} = d\mathbf{C} + dx_1 \mathbf{n} + dx_2 \mathbf{b} + x_1 d\mathbf{n} + x_2 d\mathbf{b}$$

and so for rigid motion the above gives:

$$\begin{aligned}d\mathbf{r} &= [\boldsymbol{\Omega} \times \mathbf{C} + x_1(\boldsymbol{\Omega} \times \mathbf{n}) + x_2(\boldsymbol{\Omega} \times \mathbf{b})] dt \\ &\quad + [1 - \kappa(s)x_1] ds \mathbf{t} + [dx_1 - x_2 \tau(s) ds] \mathbf{n} + [dx_2 + x_1 \tau(s) ds] \mathbf{b} \\ &= dy_1 \mathbf{i} + dy_2 \mathbf{j} + dy_3 \mathbf{k}\end{aligned}$$

where  $dy_1 = d\mathbf{r} \cdot \mathbf{i}$ ,  $dy_2 = d\mathbf{r} \cdot \mathbf{j}$  and  $dy_3 = d\mathbf{r} \cdot \mathbf{k}$ . These equations imply a  $t$  dependent coordinate transformation between  $(y_1, y_2, y_3)$  and  $(s, x_1, x_2)$ .

The following is concerned with cavities that have small circular cross-section compared with their length and are represented by a space curve

that approximates a plane circle rotating about its axis. To this end it is convenient to introduce a number of dimensionless parameters and new coordinates. First introduce polar variables  $\rho$  and  $\phi$  by

$$\begin{aligned}x_1 &= \rho \cos \phi, \\x_2 &= \rho \sin \phi\end{aligned}$$

where  $0 \leq \rho \leq \rho_0$ ,  $0 < \phi \leq 2\pi$  and  $\rho_0$  is the radius of the circular cross-section.

It is supposed that the absolute values of the curvature and torsion of the closed curve  $\mathbf{C}$  are bounded from above by  $\kappa_0$  and  $\tau_0$  respectively and that the scale of  $\mathbf{C}$  is given by that of a circle of radius  $a_0$ . Introduce the dimensionless parameters

$$\begin{aligned}\epsilon\mu_1 &= \frac{\Omega\rho_0}{c}, \\ \mu_2 &= \frac{\Omega a_0}{c}, \\ \epsilon\mu_3 &= \rho_0\kappa_0, \\ \mu_4 &= \rho_0\tau_0.\end{aligned}$$

The dimensionless parameter  $\epsilon$  indicates the order of small quantities that will be used below to approximate the metric appropriate for a cavity with small cross section. Alternative assumptions about the assignment of  $\epsilon$  to the quantities  $\{\mu_1, \mu_2, \mu_3, \mu_4\}$  will give different approximation schemes. The above choice will be shown to give the classical Sagnac beat frequency to first order in a wavetube based on a planar space curve.

The calculation will proceed for

$$d\mathbf{r} \cdot d\mathbf{r} \equiv dy_1 \otimes dy_1 + dy_2 \otimes dy_2 + dy_3 \otimes dy_3$$

to lowest order in  $\epsilon$  for a curve that approximates a circle<sup>3</sup> of radius  $a_0$  rotating with uniform angular speed  $\Omega$  about its axis. Introduce the scaled polar coordinates  $(\hat{s}, \hat{\rho}, \phi)$  and  $\hat{\lambda}$  where

$$\begin{aligned}\hat{\lambda} &= \frac{ct}{\rho_0}, \\ \hat{s} &= \frac{s}{\rho_0}, \\ \hat{\rho} &= \frac{\rho}{\rho_0}\end{aligned}$$

and the scaled quantities

$$\begin{aligned}\hat{\kappa}(\hat{s}) &= \frac{\kappa(s)}{\kappa_0}, \\ \hat{\tau}(\hat{s}) &= \frac{\tau(s)}{\tau_0}\end{aligned}$$

---

<sup>3</sup>Possibly covered more than once (see Figure 1).

and consider the class of  $\mathbf{C}$  for which

$$\begin{aligned} [\mathbf{t} \cdot (\mathbf{k} \times \mathbf{C})](s, t) &= a_0 [1 + \epsilon \Gamma_1(\hat{s}, \hat{\lambda})], \\ [\mathbf{n} \cdot (\mathbf{k} \times \mathbf{C})](s, t) &= a_0 \epsilon \Gamma_2(\hat{s}, \hat{\lambda}), \\ [\mathbf{b} \cdot (\mathbf{k} \times \mathbf{C})](s, t) &= a_0 \epsilon \Gamma_3(\hat{s}, \hat{\lambda}). \end{aligned} \tag{37}$$

Thus, to lowest (zeroth) order in  $\epsilon$

$$\frac{d\mathbf{r}}{\rho_0} = \mathbf{t} d\hat{s} + \mathbf{n} [d\hat{x}_1 - \mu_4 \hat{\tau}(\hat{s}) \hat{x}_2 d\hat{s}] + \mathbf{b} [d\hat{x}_2 + \mu_4 \hat{\tau}(\hat{s}) \hat{x}_1 d\hat{s}] + \mathbf{t} \mu_2 d\hat{\lambda}.$$

In terms of  $(\hat{s}, \hat{\rho}, \phi)$  and  $\hat{\lambda}$

$$\begin{aligned} \frac{d\mathbf{r} \cdot d\mathbf{r}}{\rho_0^2} &= (d\hat{s} + \mu_2 d\hat{\lambda}) \otimes (d\hat{s} + \mu_2 d\hat{\lambda}) \\ &\quad + \hat{\rho}^2 [d\phi + \mu_4 \hat{\tau}(\hat{s}) d\hat{s}] \otimes [d\phi + \mu_4 \hat{\tau}(\hat{s}) d\hat{s}] + d\hat{\rho} \otimes d\hat{\rho} \end{aligned}$$

and the zeroth order space curve is a circle of radius  $a_0$  orthogonal to the rotation axis  $\mathbf{k}$ .

## 5 Ring cavities on spacetime

We shall consider only stationary axisymmetric spacetimes. Thus  $(\mathcal{M}, g)$  admits a commuting pair of Killing vector fields  $K$  and  $L$ :

$$\begin{aligned} \mathcal{L}_K g &= 0, \\ \mathcal{L}_L g &= 0, \\ [K, L] &= 0 \end{aligned}$$

where  $\mathcal{L}_X$  is the Lie derivative with respect to  $X$ . The vector field  $K$  is timelike and future-pointing and the vector field  $L$  is spacelike and has closed orbits. Here by definition, material points that are “rotating”<sup>4</sup> follow

---

<sup>4</sup>There is no unique definition of “rotation” or “rigidity” in general spacetimes. Indeed there exist a plethora of possible intrinsically defined notions of “rotation” that compete for attention. Such notions are generally associated with the alternative notions of “local frames” in a generic spacetime. In the neighborhood of most events the use of timelike geodesic coordinates yield vector fields that offer a good approximation to the “inertial frames” of flat spacetime. They have natural generalisations to Fermi-Walker charts in the neighbourhood of arbitrary timelike worldlines. These are associated with Fermi-Walker parallel ortho-normal frames attached to such worldlines which may be naturally identified as constituting a “non-rotating” frame attached to such an observer. Fermi-Walker frames have the virtue that they admit an operational definition. Such notions are local and apply to spacetimes with no particular symmetries. If the spacetime has preferred timelike global (local) vector fields, such as timelike Killing vectors, they offer a field of preferred global (local) observers. Such vector fields may have vorticity that contributes to a notion of local rotation in an extended region. If there are additional spacelike

timelike worldlines whose tangents at any event are a linear combination  $V$  of  $K$  and  $L$  at that event. If the spacetime is asymptotically flat and the normalised  $V$  is timelike asymptotically it also offers a field of stationary observers.

## 5.1 Flat spacetime

Before constructing a local coframe adapted to a twisted wavetube rotating in a spacetime with gravitation we consider the simpler case of Minkowski spacetime. The metric tensor  $g$  on Minkowski spacetime is

$$\begin{aligned} g &= -c^2 dT \otimes dT + dy_1 \otimes dy_1 + dy_2 \otimes dy_2 + dy_3 \otimes dy_3 \\ &= -c^2 dT \otimes dT + d\mathbf{r} \cdot d\mathbf{r} \end{aligned}$$

in terms of the inertial coordinates  $(T, y_1, y_2, y_3)$ . It possesses the timelike future-pointing Killing vector field  $\partial/\partial T$  and the spacelike Killing vectors  $\{\partial/\partial y_1, \partial/\partial y_2, \partial/\partial y_3\}$  and  $\{L_1, L_2, L_3\}$  where

$$\begin{aligned} L_1 &= y_2 \frac{\partial}{\partial y_3} - y_3 \frac{\partial}{\partial y_2}, \\ L_2 &= y_3 \frac{\partial}{\partial y_1} - y_1 \frac{\partial}{\partial y_3}, \\ L_3 &= y_1 \frac{\partial}{\partial y_2} - y_2 \frac{\partial}{\partial y_1}. \end{aligned}$$

On the wavetube spacetime domain  $(T, y_1, y_2, y_3)$  is related to the spacetime Frenet coordinates  $(t, s, x_1, x_2)$  by

$$\begin{aligned} T &= t, \\ y_1 &= \mathbf{i} \cdot [\mathbf{C}(s, t) + x_1 \mathbf{n}(s, t) + x_2 \mathbf{b}(s, t)], \\ y_2 &= \mathbf{j} \cdot [\mathbf{C}(s, t) + x_1 \mathbf{n}(s, t) + x_2 \mathbf{b}(s, t)], \\ y_3 &= \mathbf{k} \cdot [\mathbf{C}(s, t) + x_1 \mathbf{n}(s, t) + x_2 \mathbf{b}(s, t)]. \end{aligned}$$

The wavetube apparatus follows integral curves of  $\partial/\partial t$  in spacetime. By expressing the vector field  $\partial/\partial t$  with respect to  $(T, y_1, y_2, y_3)$ :

$$\frac{\partial}{\partial t} = \frac{\partial}{\partial T} + \mathbf{i} \cdot \boldsymbol{\Omega} L_1 + \mathbf{j} \cdot \boldsymbol{\Omega} L_2 + \mathbf{k} \cdot \boldsymbol{\Omega} L_3$$

Killing fields then additional local timelike combinations may be considered as observer fields [16]. Preferences must be based on expediency within some operational framework. Sagnac interferometry offers such a framework. Many discussions of this phenomena are based on the use of ray optics and the behaviour of photons constrained to follow null non-geodesic paths by idealised mirrors. Such mirrors act as “local observers” and the particular observer field to which they belong offers a natural frame for the analysis of the experiment. In this article we concentrate on the electromagnetic field aspect and make no use of the eikonal or ray approximation. We do however require the existence of a stationary axially symmetric spacetime and hence the existence of the Killing vectors  $K$  and  $L$  above.



it can be seen that  $\partial/\partial t$  is a linear combination of the timelike future-pointing Killing vector field  $K = \partial/\partial T$  and the spacelike Killing vector field  $L$ :

$$L = \mathbf{i} \cdot \boldsymbol{\Omega} L_1 + \mathbf{j} \cdot \boldsymbol{\Omega} L_2 + \mathbf{k} \cdot \boldsymbol{\Omega} L_3$$

where  $[K, L] = 0$ .

At the instant  $t = t_0$  write  $\mathbf{C}$  in the form

$$\mathbf{C}(s, t_0) = \boldsymbol{\Gamma}_{t_0}(s) + \epsilon \boldsymbol{\gamma}(s, t_0)$$

where  $\boldsymbol{\Gamma}_{t_0}$  is a plane circle in  $\mathbf{R}^3$  rotating with angular speed  $\Omega$  about its axis  $\mathbf{k}$ . The curve image  $\boldsymbol{\Gamma}_{t_0}(s)$  has tangent  $\mathbf{T}_{t_0}(s)$ , normal  $\mathbf{N}_{t_0}(s)$ , constant binormal  $\mathbf{B}_{t_0}(s) = \mathbf{k}$  and radius  $a_0$ . Note that  $s$  is *not* necessarily the arc parameter of  $\boldsymbol{\Gamma}_{t_0}$ .

The vector  $\boldsymbol{\Gamma}_{t_0}(s)$  can be expressed

$$\boldsymbol{\Gamma}_{t_0}(s) = -a_0 \mathbf{N}_{t_0}(s)$$

and it is supposed that the tangent  $\mathbf{t}$ , normal  $\mathbf{n}$  and binormal  $\mathbf{b}$  of  $\mathbf{C}$  satisfy

$$\begin{aligned} \mathbf{t}(s, t) &= \mathbf{T}_t(s) + O(\epsilon), \\ \mathbf{n}(s, t) &= \cos[\beta(s, t)] \mathbf{N}_t(s) + \sin[\beta(s, t)] \mathbf{B}_t(s) + O(\epsilon), \\ \mathbf{b}(s, t) &= -\sin[\beta(s, t)] \mathbf{N}_t(s) + \cos[\beta(s, t)] \mathbf{B}_t(s) + O(\epsilon) \end{aligned} \quad (38)$$

for some angle  $\beta(s, t)$ . Using

$$\begin{aligned} \mathbf{T} \cdot \mathbf{k} &= 0, \\ \mathbf{B} &= \mathbf{k} \end{aligned}$$

it follows that

$$\begin{aligned} \mathbf{t} \cdot (\mathbf{k} \times \mathbf{C})(s, t) &= a_0 + O(\epsilon), \\ \mathbf{n} \cdot (\mathbf{k} \times \mathbf{C})(s, t) &= O(\epsilon), \\ \mathbf{b} \cdot (\mathbf{k} \times \mathbf{C})(s, t) &= O(\epsilon) \end{aligned}$$

which is consistent with (37). Thus, in terms of  $(t, s, x_1, x_2)$  the metric tensor  $g$  is

$$\begin{aligned} g &= -e^0 \otimes e^0 + e^1 \otimes e^1 + e^2 \otimes e^2 + e^3 \otimes e^3 + O(\epsilon), \\ e^0 &= \rho_0 d\hat{\lambda} = c dt, \\ e^1 &= \rho_0 (d\hat{s} + \mu_2 d\hat{\lambda}) = ds + \Omega a_0 dt, \\ e^2 &= \rho_0 d\hat{\rho} = d\rho, \\ e^3 &= \rho_0 \hat{\rho} [d\phi + \mu_4 \hat{\tau}(\hat{s}) d\hat{s}] = \rho [d\phi + \tau(s) ds]. \end{aligned} \quad (39)$$

where  $\{e^0, e^1, e^2, e^3\}$  is orthonormal to lowest order in  $\epsilon$ . Note that the approximate Minkowski metric is insensitive to  $\mu_3$  and the curvature of  $\mathbf{C}$ .

## 5.2 Slowly rotating Kerr spacetime

The metric tensor at large distances from an isolated compact rotating body in an asymptotically flat spacetime, with Newtonian gravitational mass  $M$  and angular momentum  $J$ , may be approximated (for  $r \gg 2G_N M/c^2$  where  $G_N$  is Newton's gravitational constant) by

$$\begin{aligned}
 g = & -c^2 \left( 1 - \frac{2G_N M}{rc^2} \right) dT \otimes dT \\
 & + \left( 1 + \frac{2G_N M}{rc^2} \right) (dr \otimes dr + r^2 d\theta \otimes d\theta + r^2 \sin^2 \theta d\varphi \otimes d\varphi) \\
 & - \frac{2G_N J}{rc^2} \sin^2 \theta (d\varphi \otimes dT + dT \otimes d\varphi)
 \end{aligned} \quad (40)$$

in spherical polar coordinates  $(T, r, \theta, \varphi)$ .

The use of the metric (40) is of course an idealisation for physical applications such as terrestrial ring lasers, where one does not have two Killing vectors. In particular, due to interactions with other celestial bodies the positions of both the rotation and angular momentum axes will not quite coincide with each other and their positions will vary with time. As reported in ref. [5] for the case of ring lasers at the Earth's surface such effects are three to four orders of magnitude larger than the Lense-Thirring effect. Nonetheless the calculation presented here serves a useful purpose in isolating effects due to gravito-magnetism. The implications of time variation of the rotation and angular momentum axes of the Earth on terrestrial Lense-Thirring measurements will be discussed elsewhere [15].

The vector fields  $\partial/\partial T$  and  $\partial/\partial\varphi$  are a commuting pair of Killing vectors. Furthermore,  $K = \partial/\partial T$  is timelike and future-pointing and  $L = \Omega \partial/\partial\varphi$  is spacelike and has closed orbits. Consider the acceleration of matter on one of the integral curves of the 4-velocity field  $V = (K + L)/\sqrt{-g(K + L, K + L)}$  with respect to a stationary observer belonging to the 4-velocity field  $W = K/\sqrt{-g(K, K)}$ . At events where the integral curves of  $V$  and  $W$  coincide  $V$  has spatial acceleration  $\mathcal{A} = H_W(\nabla_V V)$  where  $H_W \equiv 1 + W \otimes \tilde{W}$  projects the 4-acceleration to the instantaneous 3-space of  $W$ . In the non-relativistic weak gravitational field limit one finds that the g-orthonormal components of  $\mathcal{A}$  yield a centripetal acceleration with dominant magnitude  $r_0 \Omega^2$  at an event with coordinates  $r = r_0, \theta = \pi/2$ . Thus each observer within  $W$  would interpret such events within  $V$  to have instantaneous 3-acceleration produced by rotation with angular speed  $\Omega$ .

The asymptotically Minkowski coordinate chart  $(T, y_1, y_2, y_3)$  is given in terms of  $(T, r, \theta, \varphi)$  as

$$\begin{aligned}
 y_1 &= r \sin \theta \cos \varphi, \\
 y_2 &= r \sin \theta \sin \varphi, \\
 y_3 &= r \cos \theta.
 \end{aligned}$$

The dot  $\mathbf{x} \cdot \mathbf{y}$  and cross  $\mathbf{x} \times \mathbf{y}$  products of the pair of vectors  $\{\mathbf{x}, \mathbf{y}\}$  are defined with respect to the tensor  $h$ :

$$h = dy_1 \otimes dy_1 + dy_1 \otimes dy_1 + dy_2 \otimes dy_2 + dy_3 \otimes dy_3$$

and the  $h$ -orthonormal frame  $(\mathbf{i}, \mathbf{j}, \mathbf{k})$ :

$$\begin{aligned}\mathbf{i} &= \frac{\partial}{\partial y_1}, \\ \mathbf{j} &= \frac{\partial}{\partial y_2}, \\ \mathbf{k} &= \frac{\partial}{\partial y_3}\end{aligned}$$

and, as before, the vector  $\mathbf{r}_T$ ,

$$\mathbf{r}_T = y_1 \mathbf{i} + y_2 \mathbf{j} + y_3 \mathbf{k},$$

locates the point  $(T, y_1, y_2, y_3)$ .

The metric tensor  $g$  has the form

$$\begin{aligned}g &= -c^2 \left( 1 - \frac{2G_N M}{rc^2} \right) dT \otimes dT + \left( 1 + \frac{2G_N M}{rc^2} \right) d\mathbf{r} \cdot d\mathbf{r} \\ &\quad - \frac{2G_N J}{r^3 c^2} \left[ \mathbf{k} \cdot (\mathbf{r} \times d\mathbf{r}) \otimes dT + dT \otimes \mathbf{k} \cdot (\mathbf{r} \times d\mathbf{r}) \right]\end{aligned}$$

where  $(T, y_1, y_2, y_3)$  and the spacetime coordinates  $(t, \underline{s}, \underline{x}_1, \underline{x}_2)$  satisfy

$$\begin{aligned}T &= t, \\ y_1 &= \mathbf{i} \cdot [\mathbf{C}(\underline{s}, t) + \underline{x}_1 \mathbf{n}(\underline{s}, t) + \underline{x}_2 \mathbf{b}(\underline{s}, t)], \\ y_2 &= \mathbf{j} \cdot [\mathbf{C}(\underline{s}, t) + \underline{x}_1 \mathbf{n}(\underline{s}, t) + \underline{x}_2 \mathbf{b}(\underline{s}, t)], \\ y_3 &= \mathbf{k} \cdot [\mathbf{C}(\underline{s}, t) + \underline{x}_1 \mathbf{n}(\underline{s}, t) + \underline{x}_2 \mathbf{b}(\underline{s}, t)]\end{aligned}$$

and the  $h$ -orthonormal frame  $(\mathbf{t}, \mathbf{n}, \mathbf{b})$  solves the Frenet-Serret equations

$$\begin{aligned}\mathbf{t} &= \frac{\partial}{\partial \underline{s}} \mathbf{C}, \\ \frac{\partial}{\partial \underline{s}} \mathbf{t} &= \underline{\kappa} \mathbf{n}, \\ \frac{\partial}{\partial \underline{s}} \mathbf{n} &= -\underline{\kappa} \mathbf{t} + \underline{\tau} \mathbf{b}, \\ \frac{\partial}{\partial \underline{s}} \mathbf{b} &= -\underline{\kappa} \mathbf{n}.\end{aligned}$$

The functions  $\{\underline{s}, \underline{x}_1, \underline{x}_2, \underline{\kappa}, \underline{\tau}\}$  are underlined as a reminder that they are normalized with respect to the tensor  $h$  rather than the spacetime metric  $g$ .

As in the previous section consider curves of the form

$$\mathbf{C}(\underline{s}, t) = \mathbf{\Gamma}_t(\underline{s}) + \epsilon \boldsymbol{\gamma}(\underline{s}, t)$$

subject to (38), with  $s$  replaced by  $\underline{s}$ , where  $\mathbf{\Gamma}_t(\underline{s})$  is the rotating plane circle of  $h$ -radius  $a_0$  centred at the point  $\mathbf{r}_T = z_0 \mathbf{k}$ ,  $z_0 > 0$  with the Frenet frame  $\{\mathbf{T}, \mathbf{N}, \mathbf{B}\}$  and  $\boldsymbol{\Omega} = \Omega \mathbf{k}$ . Here one is considering  $O(\epsilon)$  perturbations about a ‘‘circular’’ space curve parallel to the ‘‘equatorial plane’’ of the Kerr geometry where elements of the wavetube apparatus follow integral curves of  $\partial/\partial t = \partial/\partial T + \Omega \partial/\partial \varphi$  in this spacetime.

As before, introduce the dimensionless functions

$$\begin{aligned} \hat{\underline{s}} &= \frac{\underline{s}}{\rho_0}, \\ \hat{x}_1 &= \frac{x_1}{\rho_0}, \\ \hat{x}_2 &= \frac{x_2}{\rho_0}, \\ \hat{\kappa}(\hat{\underline{s}}) &= \frac{\kappa(\underline{s})}{\kappa_0}, \\ \hat{\tau}(\hat{\underline{s}}) &= \frac{\tau(\underline{s})}{\tau_0}. \end{aligned}$$

Since

$$\mathbf{\Gamma}_t(\underline{s}) = -a_0 \mathbf{N}_t(\underline{s})$$

and the position vector  $\mathbf{r}$  has the form

$$\mathbf{r} = -a_0 [\mathbf{N} + O(\epsilon)]$$

and using

$$\begin{aligned} \frac{d\mathbf{r}}{\rho_0} &= \mathbf{t} d\hat{\underline{s}} + \mathbf{n} [d\hat{x}_1 - \mu_4 \hat{\tau}(\hat{\underline{s}}) \hat{x}_2 d\hat{\underline{s}}] + \mathbf{b} [d\hat{x}_2 + \mu_4 \hat{\tau}(\hat{\underline{s}}) \hat{x}_1 d\hat{\underline{s}}] + \mathbf{t} \mu_2 d\hat{\lambda}, \\ \mathbf{B} &= \mathbf{k} \end{aligned}$$

with (38) it follows that

$$\mathbf{k} \cdot (\mathbf{r} \times d\mathbf{r}) = \rho_0 a_0 [d\hat{\underline{s}} + \mu_2 d\hat{\lambda} + O(\epsilon)].$$

The metric tensor  $g$  adapted to  $\mathbf{C}$  is

$$\begin{aligned} g/\rho_0^2 &= -(1 - \mu_5) d\hat{\lambda} \otimes d\hat{\lambda} + (1 + \mu_5) [(d\hat{\underline{s}} + \mu_2 d\hat{\lambda}) \otimes (d\hat{\underline{s}} + \mu_2 d\hat{\lambda}) \\ &\quad + \hat{\rho}^2 (d\phi + \mu_4 \hat{\tau}(\hat{\underline{s}}) d\hat{\underline{s}}) \otimes (d\phi + \mu_4 \hat{\tau}(\hat{\underline{s}}) d\hat{\underline{s}}) + d\hat{\rho} \otimes d\hat{\rho}] \\ &\quad - \mu_6 [(d\hat{\underline{s}} + \mu_2 d\hat{\lambda}) \otimes d\hat{\lambda} + d\hat{\lambda} \otimes (d\hat{\underline{s}} + \mu_2 d\hat{\lambda})] \end{aligned} \quad (41)$$

to lowest order in  $\epsilon$  where

$$\begin{aligned} r_0 &= \sqrt{a_0^2 + z_0^2}, \\ \mu_5 &= \frac{2G_N M}{r_0 c^2}, \\ \mu_6 &= \frac{2G_N J a_0}{r_0^3 c^3} \end{aligned}$$

and

$$\begin{aligned} \underline{x}_1 &= \underline{\rho} \cos \phi, \\ \underline{x}_2 &= \underline{\rho} \sin \phi. \end{aligned}$$

A  $g$ -orthonormal coframe to lowest order in  $\epsilon$  is

$$\begin{aligned} e^0 &= [1 - \mu_5 + \mu_6^2/(1 + \mu_5)]^{1/2} c dt, \\ e^1 &= [(1 + \mu_5)^{1/2} \mu_2 - \mu_6/(1 + \mu_5)^{1/2}] c dt + ds, \\ e^2 &= d\rho, \\ e^3 &= \rho [d\phi + \tau(s) ds] \end{aligned} \tag{42}$$

where

$$\begin{aligned} s &= (1 + \mu_5)^{1/2} \underline{s}, \\ \rho &= (1 + \mu_5)^{1/2} \underline{\rho}, \\ \tau(s) &= (1 + \mu_5)^{-1/2} \underline{\tau}(\underline{s}). \end{aligned} \tag{43}$$

## 6 Twisting EM modes on spacetime

Both coframes (39) and (42) satisfy (2) and so single-valued propagating electromagnetic  $F$  modes inside a wavetube with circular cross-section of radius  $\rho_0$  can be generated from particular solutions of the Helmholtz equations discussed earlier. Solutions regular in the wavetube follow from the forms  $J_n(|\alpha|\rho) \exp[in\chi(\phi, s)]$  where  $n \in \mathbf{Z}$ ,

$$\chi(s, \phi) = \phi + \int_0^s \tau(\sigma) d\sigma$$

and  $\alpha = \alpha_{TM}$  or  $\alpha = \alpha_{TE}$  (see equations (34)). The role of the Frenet torsion in solutions of the scalar Helmholtz equation in coordinates adapted to non-planar curves has been noted before in a number of different contexts [10, 11, 12].

The  $F_{TM}$  and  $F_{TE}$  modes follow from

$$\Phi(s, \rho, \phi) = J_n(|\alpha_{TM}|\rho) \exp[in\chi(\phi, s)]$$

with  $\alpha_{TM}$  satisfying

$$J_n(|\alpha_{TM}|\rho_0) = 0$$

and

$$\Psi(s, \rho, \phi) = J_n(|\alpha_{TE}|\rho) \exp[in\chi(\phi, s)]$$

with  $\alpha_{TE}$  satisfying

$$J'_n(|\alpha_{TE}|\rho_0) = 0$$

where  $J_n(x)$  is the  $n$ th regular Bessel function of the first kind and  $J'_n(x) = dJ_n(x)/dx$ .

For both TE and TM modes

$$\xi = -\omega_\xi dt + k_\xi ds \quad (44)$$

and, using  $V = \partial_t / \sqrt{-g(\partial_t, \partial_t)}$ ,

$$\begin{aligned} \nu_\xi &= \frac{c}{2\pi} \xi(V) \\ &= \frac{c\omega_\xi}{2\pi \sqrt{-g(\partial_t, \partial_t)}} \end{aligned}$$

is the frequency (Hz), measured by the wavetube apparatus, of the field mode associated with  $\xi = dW_{TM}$  or  $\xi = dW_{TE}$ . Positive wavenumbers  $k_\xi$  correspond to propagation in the direction of the tangent  $\mathbf{t}$  and negative wavenumbers to propagation in the opposite direction.

Since the wavetube is closed, i.e. the wavetube interior on spacetime is topologically  $\mathbf{R} \times S^1 \times \mathbf{D}$ , the Maxwell 2-form satisfies

$$F(t, s, \rho, \phi) = F(t, s + l, \rho, \phi),$$

where  $l$  is the length of the wavetube and so using (44) and either (32) or (33)

$$k[N, n] \equiv k_\xi = \frac{2\pi N}{l} - n\bar{\tau}, \quad N \in \mathbf{Z} \quad (45)$$

where

$$\bar{\tau} \equiv \frac{1}{l} \int_0^l \tau(s) ds$$

is the average Frenet torsion. The mode spectrum is classified using the triple of integers  $(N, p, n)$ , where the positive integer  $p$  labels a solution of  $J_n(|\alpha_{TM}|\rho_0) = 0$  in the TM case or  $J'_n(|\alpha_{TE}|\rho_0) = 0$  in the TE case.

## 6.1 Frequency spectra

The longitudinal members of (39) and (42) have the form

$$\begin{aligned} e^0 &= A dt, \\ e^1 &= B dt + ds \end{aligned}$$

where  $A$  and  $B$  are constants with the dimensions of  $c$ . For each  $|\alpha| = \zeta/\rho_0$ , where  $\alpha = \alpha_{TM}$  or  $\alpha = \alpha_{TE}$  (see equations (34)) and  $\zeta$  is determined by the boundary conditions, the dispersion relation  $g^{-1}(\alpha, \alpha) = -|\alpha|^2$  with  $\omega_\xi > 0$  yields

$$\omega_\xi = \frac{\sqrt{A^2 - B^2}}{A^2 \mathcal{N}^2 - B^2} \left[ -B \mathfrak{K} + \sqrt{B^2 \mathfrak{K}^2 + (A^2 \mathcal{N}^2 - B^2)(\mathfrak{K}^2 + A^2 \zeta^2 / \rho_0^2)} \right] \quad (46)$$

where

$$\mathfrak{K} = k \sqrt{A^2 - B^2}.$$

It is assumed that, for terrestrial applications,  $|B|/A < \mathcal{N}$  and so the sign of the square root of the discriminant in (46) is chosen to be positive. In addition to  $k \equiv k[N, n]$  introduce the scalars  $\{\omega_T, \zeta_T\}$  dependent on the mode indices  $(N, p, n)$  and the type  $T \in \{TE, TM\}$  as follows:

$$\begin{aligned} \omega_\xi &\equiv \omega_T = \omega_T[N, p, n], \\ \zeta_T &\equiv \zeta_T[p, n] \end{aligned}$$

where  $J_n(\zeta_{TM}[p, n]) = 0$  and  $J'_n(\zeta_{TE}[p, n]) = 0$ . The wavetube apparatus measures the frequency

$$\nu_T[N, p, n] = \frac{c}{2\pi} dW_T(V)$$

and so here

$$\nu_T[N, p, n] = \frac{\omega_T[N, p, n]c}{2\pi\sqrt{A^2 - B^2}}. \quad (47)$$

We may approximate this expression further by taking into account the relative magnitudes of  $N$ ,  $n$ ,  $l\bar{\tau}$ ,  $\zeta_T$  and  $k\rho_0$ . For a lasing medium excited by a RF field  $|N| \gg 1$  is expected and it is assumed that  $2\pi|N|/l \gg |n\bar{\tau}|$  and  $2\pi|N|/l \gg |\zeta_T|/\rho_0$ . Then (46) has the form

$$\omega_T[N, p, n] \simeq \frac{|k[N, n](A^2 - B^2)}{A\mathcal{N} + \text{sgn}(k[N, n])B} \quad (48)$$

where

$$\text{sgn}(k) = \begin{cases} -1 & \text{if } k < 0, \\ +1 & \text{if } k \geq 0. \end{cases}$$

Using (45) and  $2\pi|N|/l > |n\bar{\tau}|$  it follows that  $\text{sgn}(k) = \text{sgn}(N)$  hence

$$|k| = \frac{2\pi|N|}{l} - \text{sgn}(N)n\bar{\tau}. \quad (49)$$

Note that  $\omega_T$  and  $\nu_T$  are independent of the mode type  $T$  and the Bessel root index  $p$  in this approximation. Henceforth we write  $\omega = \omega_T$  and  $\nu = \nu_T$  and drop their  $p$  dependencies.

For terrestrial applications we expect that  $|B|/A \ll 1$  (as well as  $|B|/A < \mathcal{N}$ ). In this case (47) becomes

$$\nu[N, n] \simeq \frac{c|N|}{l\mathcal{N}} - \text{sgn}(N) \left[ \frac{c|N|}{l} \frac{B}{A\mathcal{N}^2} + \frac{cn\bar{\tau}}{2\pi\mathcal{N}} \right] \quad (50)$$

where (49) and (48) have been used.

## 7 Multiple mode excitations and beating

If a number of electromagnetic modes of similar frequency are active in the wavetube then the time histories of the electromagnetic fields measured by the wavetube apparatus will exhibit beating. The classical [3, 4] Sagnac beat frequency  $\delta\nu_{\text{Sagnac}}$  induced by rotation on flat spacetime follows from (50) with  $\mathcal{N} \simeq 1$  and by choosing a pair of rotationally symmetric ( $n = 0$ ) modes that differ only in their directions of propagation and have  $N > 0$ :

$$\begin{aligned} \delta\nu_{\text{Sagnac}} &\equiv \nu[N, 0] - \nu[-N, 0] \\ &\simeq -\frac{2\Omega N a_0}{l} \end{aligned} \quad (51)$$

where  $A$  and  $B$  have been obtained from (39). To reveal the classical expression for the Sagnac beat frequency the parameters  $a_0$  and  $l$  and the mode index  $N$  are eliminated by introducing the area  $\mathcal{A} \equiv \pi a_0^2$  and perimeter  $\mathcal{P} \equiv 2\pi a_0$  of the plane circle approximated by the wavetube locus and the lasing wavelength  $\lambda \equiv l/N$ . It follows that

$$\delta\nu_{\text{Sagnac}} \simeq -\frac{4\Omega\mathcal{A}}{\lambda\mathcal{P}}. \quad (52)$$

### 7.1 Twisted mode beating on flat spacetime

The most general frequency difference is constructed from a pair of modes of type  $T_1, T_2 \in \{TM, TE\}$  with indices  $(N_1, p_1, n_1)$  and  $(N_2, p_2, n_2)$ . In the approximation introduced earlier we only need consider  $N$  and  $n$  dependencies:

$$\delta\nu[N_1, n_1; N_2, n_2] \equiv \nu[N_1, n_1] - \nu[N_2, n_2].$$



Thus, with  $N > 0$ , (52) has the generalization

$$\delta\nu[N, n; -N, n] \simeq -\frac{2N\Omega a_0}{l\mathcal{N}^2} - \frac{cn\bar{\tau}}{\pi\mathcal{N}}. \quad (53)$$

For terrestrial applications the external RF field generates counter- and co-propagating modes with indices  $N_1$  and  $N_2$  whose magnitudes are so large it is possible that  $|N_1| \neq |N_2|$ . More generally, there is no reason to assume that  $(|N_1|, p_1, n_1, T_1)$  and  $(|N_2|, p_2, n_2, T_2)$  are identical. With  $N_1 > 0$  and  $N_2 < 0$  and using (50) it follows that

$$\begin{aligned} \delta\nu[N_1, n_1; N_2, n_2] \simeq & \frac{c}{l\mathcal{N}}(N_1 + N_2) - \frac{a_0\Omega}{l\mathcal{N}^2}(N_1 - N_2) \\ & - \frac{c\bar{\tau}}{2\pi\mathcal{N}}(n_1 + n_2). \end{aligned}$$

## 7.2 Twisted mode beating on slowly rotating Kerr spacetime

The dimensionless parameters  $\{\mu_2, \mu_6\}$ ,

$$\begin{aligned} \mu_2 &= \frac{a_0\Omega}{c}, \\ \mu_6 &= \frac{2G_N J a_0}{r_0^3 c^3}, \end{aligned}$$

contain the *Euclidean* radius  $a_0$  of the multiply-wound plane circle  $\Gamma$  that approximates the wavelocus on Kerr spacetime  $(\mathcal{M}, g)$ . One may eliminate the parameter  $a_0$  in favour of a length determined by the spacetime metric  $g$  rather than the Euclidean metric  $d\mathbf{r} \cdot d\mathbf{r}$ .

For each constant  $(T_0, r_0, \theta_0)$  the multiply-wound planar circle may be described as the image of the map

$$\begin{aligned} \Gamma : [0, 2\pi m] &\rightarrow \mathcal{M} \\ u &\mapsto (T = T_0, r = r_0, \theta = \theta_0, \varphi = u) \end{aligned} \quad (54)$$

where  $(T, r, \theta, \varphi)$  are the coordinates used in (40),  $a_0 = r_0 \sin \theta_0$  and the positive integer  $m$  is a winding number. The arclength  $l_0$  of  $\Gamma$  is

$$l_0 \equiv \int_0^{2\pi m} \sqrt{g(\Gamma', \Gamma')} du \quad (55)$$

where  $\Gamma' = \partial_\varphi$  is tangent to  $\Gamma$ . Using (40), (54) and (55) it follows that

$$a_0 = \frac{l_0}{2\pi m} \frac{1}{\sqrt{1 + \mu_5}} \quad (56)$$

where

$$\mu_5 = \frac{2G_N M}{r_0 c^2}.$$

Introduce dimensionless parameters  $\{\mu'_2, \mu'_6\}$

$$\begin{aligned}\mu'_2 &\equiv \frac{\Omega}{c} \frac{l_0}{2\pi m}, \\ \mu'_6 &\equiv \frac{2G_N J}{r_0^3 c^3} \frac{l_0}{2\pi m}\end{aligned}$$

so that, by using (56) to eliminate  $a_0$ :

$$\begin{aligned}\mu_2 &= \frac{\mu'_2}{\sqrt{1 + \mu_5}}, \\ \mu_6 &= \frac{\mu'_6}{\sqrt{1 + \mu_5}}.\end{aligned}$$

Typically, for terrestrial applications, the magnitudes of the dimensionless parameters  $\{\mu_2, \mu'_5, \mu'_6\}$  are much less than unity. Thus, it is reasonable to approximate  $B/A$  by a polynomial obtained from the multivariate Taylor expansion of  $B/A$  with respect  $(\mu_2, \mu'_5, \mu'_6)$  about  $(0, 0, 0)$ . However, when truncating the Taylor expansion the numerical values of the terms in the series must be carefully scrutinized. For example, the parameters associated with a wavetube whose locus approximates  $\mathbf{\Gamma}$  with “radius”  $l_0/(2\pi m) \simeq 150$  m fixed on the Earth and centred on the poles have magnitudes  $|\mu'_2| \simeq 3.6 \times 10^{-11}$ ,  $|\mu_5| \simeq 1.4 \times 10^{-9}$  and  $|\mu'_6| \simeq 1.7 \times 10^{-20}$ . For terrestrial conditions  $|\mu'_2 \mu_5| > |\mu'_6|$  is generally true. It follows that

$$\frac{B}{A} \simeq \mu'_2 + \frac{1}{2} \mu'_2 \mu_5 - \mu'_6 \quad (57)$$

is a good approximation (the other terms in the Taylor series are about 10 orders of magnitude smaller).

Using (50) and (57) it follows that

$$\nu[N, n] \simeq \frac{c|N|}{l\mathcal{N}} - \text{sgn}(N) \left[ \frac{l_0}{2\pi m} \frac{\Omega|N|}{l\mathcal{N}^2} \left( 1 + \frac{G_N M}{r_0 c^2} - \frac{2G_N J}{\Omega r_0^3 c^2} \right) + \frac{cn\bar{\tau}}{2\pi\mathcal{N}} \right] \quad (58)$$

and, more generally, for a pair of modes with indices  $(N_1, n_1)$  and  $(N_2, n_2)$ , where  $N_1 > 0$  and  $N_2 < 0$ ,

$$\begin{aligned}\delta\nu[N_1, n_1; N_2, n_2] &\simeq \frac{c}{l\mathcal{N}} (N_1 + N_2) \\ &\quad - \frac{l_0}{2\pi m} \frac{\Omega}{l\mathcal{N}^2} \left[ 1 + \frac{G_N M}{r_0 c^2} - \frac{2G_N J}{\Omega r_0^3 c^2} \right] (N_1 - N_2) \quad (59) \\ &\quad - \frac{c\bar{\tau}}{2\pi\mathcal{N}} (n_1 + n_2).\end{aligned}$$

By choosing a pair of rotationally symmetric ( $n = 0$ ) modes that differ only in their directions of propagation and have  $N_1 = -N_2 = N > 0$  we find

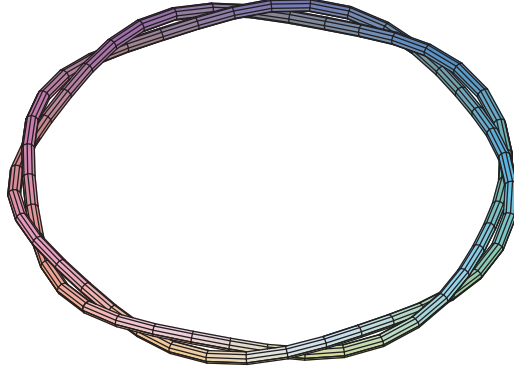


Figure 1: A 3-dimensional diagram of the type  $(2, 9; 150, 5, 5)$  torus knot.

the classical Sagnac beat frequency (52) is modified in this approximation to

$$\begin{aligned} \delta\nu_{\text{Sagnac}} &= \nu[N, 0] - \nu[-N, 0] \\ &\simeq -\frac{1}{\mathcal{N}^2} \frac{4\Omega\mathcal{A}}{\lambda\mathcal{P}} \left[ 1 + \frac{G_N M}{r_0 c^2} - \frac{2G_N J}{\Omega r_0^3 c^2} \right] \end{aligned} \quad (60)$$

where the “area”  $\mathcal{A}$  and “perimeter”  $\mathcal{P}$  of  $\mathbf{\Gamma}$  are defined as

$$\begin{aligned} \mathcal{A} &\equiv \frac{l_0^2}{4\pi m^2}, \\ \mathcal{P} &\equiv \frac{l_0}{m} \end{aligned}$$

in terms of total arclength  $l_0$  and winding number  $m$  of  $\mathbf{\Gamma}$  and  $\lambda = l_0/N$ .

Using (43) it can be seen that the average torsion  $\bar{\tau}$  is related to the Euclidean torsion  $\tau(\underline{s})$  of the wavetube locus by

$$\bar{\tau} = \frac{1}{\sqrt{1 + \mu_5}} \frac{1}{\underline{l}} \int_0^{\underline{l}} \tau(\underline{s}) d\underline{s}$$

where  $\underline{l} \equiv l/\sqrt{1 + \mu_5}$ .

### 7.3 Example

To illustrate the significance of the Frenet torsion contribution to (53) we consider a wavetube based on a particular torus knot. A type  $(u_1, u_2; v_1, v_2, v_3)$  torus knot is a curve  $\mathbf{C}$  specified by a pair of integers  $(u_1, u_2) \in \mathbf{Z}^2$  and a

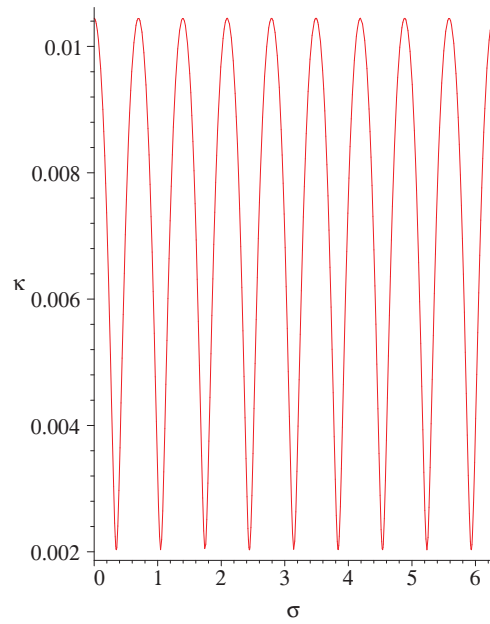


Figure 2a: The Euclidean Frenet curvature  $\underline{\kappa}$  of the type  $(2, 9; 150, 5, 5)$  torus knot. Note that the abscissa is labeled by  $\sigma$  and not the Euclidean arclength  $\underline{s}$  (see main text).

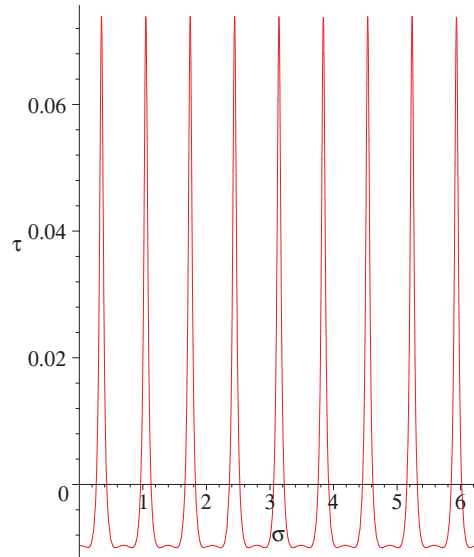


Figure 2b: The Euclidean Frenet torsion  $\underline{\tau}$  of the type  $(2, 9; 150, 5, 5)$  torus knot. Note that the abscissa is labeled by  $\sigma$  and not the Euclidean arclength  $\underline{s}$  (see main text).

triple of real numbers  $(v_1, v_2, v_3) \in \mathbf{R}^3$  :

$$\begin{aligned}\mathbf{\Gamma} &: \sigma \rightarrow [\mathbf{\Gamma}_1(\sigma), \mathbf{\Gamma}_2(\sigma), \mathbf{\Gamma}_3(\sigma)] \\ \mathbf{\Gamma}_1(\sigma) &= \mathbf{i} \cdot \mathbf{\Gamma}(\sigma) = [v_1 + v_2 \cos(u_2\sigma)] \cos(u_1\sigma), \\ \mathbf{\Gamma}_2(\sigma) &= \mathbf{j} \cdot \mathbf{\Gamma}(\sigma) = [v_1 + v_2 \cos(u_2\sigma)] \sin(u_1\sigma), \\ \mathbf{\Gamma}_3(\sigma) &= \mathbf{k} \cdot \mathbf{\Gamma}(\sigma) = v_3 \sin(u_2\sigma), \\ \mathbf{C}(\underline{s}) &= \mathbf{\Gamma}(\sigma(\underline{s}))\end{aligned}$$

where the Euclidean arc parameter  $\underline{s}$  satisfies

$$\frac{d\mathbf{C}}{d\underline{s}} \cdot \frac{d\mathbf{C}}{d\underline{s}} = 1.$$

The torus knot  $\mathbf{C}$  is approximated by a multiply-wound circle of Euclidean radius  $a_0 = v_1$ .

The type  $(2, 9; 150, 5, 5)$  torus knot is shown in figure 1 and its Frenet curvature and torsion are shown in figures 2a and 2b. Choosing MKS units, so  $a_0 = v_1 = 150$  m, this particular knot has  $\bar{\tau} = 3.13 \times 10^{-4} \text{ m}^{-1}$  and so  $cn\bar{\tau}/\pi = n29.8$  kHz. The classical Sagnac beat frequency (52) of a circular He-Ne wavetube laser ( $\lambda = 633$  nm) and “radius” 150 m fixed on the Earth ( $\Omega = 7.29 \times 10^{-5}$  rad/s) and centred on the poles is 34.5 kHz. Clearly, for  $n = 1$  and  $\mathcal{N} \simeq 1$  the standard Sagnac and torsion contributions to the beat frequency are quite similar and, moreover, in order to determine  $\Omega$  from the beat frequency both contributions would have to be taken into account.

## Conclusions

A particular approximation scheme has been developed that permits one to determine the electromagnetic mode structure for a rotating slender wavetube containing a non-conducting isotropic homogeneous dispersionless medium. The possible effects of a weak non-Newtonian gravito-magnetic field on these modes has been included. The approximation enables one to identify TE and TM type field configurations with respect to the longitudinal axis of the wavetube. Although this need not be fixed in space, provided the dimensionless parameters  $\mu_1$  and  $\mu_3$  are smaller than  $\mu_2$  the decomposition remains valid to the order prescribed. In this regime one finds that such a wavetube with non-zero integrated Frenet torsion can produce a modification to the classical Sagnac beat frequency due to any rotation of the interferometer.

To detect effects of gravito-magnetism in this scenario one must adjust the parameters  $\{l_0, \Omega, \rho_0, \tau_0, \kappa_0\}$  so that the effects due to the dimensionless parameters  $\{\mu_5, \mu'_6\}$  can be distinguished experimentally from those produced by  $\{\mu_1, \mu'_2, \mu_3\}$ . There are of course practical limitations that bound  $l_0$  and  $\rho_0$  and the possibility of increasing  $\Omega$  by rotating the interferometer.

Furthermore the example given in section 7.1 shows that there exist slender geometrical structures based on space curves having small Frenet curvature but integrated Frenet torsion giving rise to interference effects commensurate with those produced by the rotation of the Earth. It is difficult to construct geometrical configurations that meet all the above competing constraints needed to reveal terrestrial gravito-magnetic effects without releasing the condition of relatively constant local Frenet curvature.

To overcome this limitation it is clear that a more complete analysis of the mode spectra should take into account perturbations induced by variations of Frenet curvature of the wavetube. This is a non-trivial modification since it implies that the Maxwell equations no longer separate into twisted TE and TM modes. However, for appropriate local curvature variations one may extend the approximation scheme using a perturbation approach and the basis of twisted modes found in this analysis. This would yield a clear separation of the effects of Frenet torsion and Frenet curvature on the Sagnac beat frequency. Such developments would provide a more complete picture of the delicate interplay between acceleration, geometry, electromagnetism and gravity that arises in any attempt to design an effective ring-laser capable of detecting terrestrial gravito-magnetism.

## Acknowledgements

DAB, AN and RWT are most grateful for the hospitality provided by the Department of Physics and Astronomy, University of Canterbury, Christchurch, New Zealand and for valuable discussions with G Stedman, R Hurst and R Reeves. They are also grateful to M Hamilton, University of Adelaide, for information on optical polarising devices. DAB acknowledges financial support from the Royal Society, DLW from the Marsden fund of the Royal Society of New Zealand and RWT is grateful to BAe Systems for their support and interest in this research.

## References

- [1] Sagnac G., C. R. Acad. Sci. **157**, 708 (1913); **157**, 1410 (1913).
- [2] Post E. J., Rev. Mod. Phys. **39**, 475 (1967).
- [3] Anderson R., Bilger H. R., Stedman G. E., Am. J. Phys. **62** (11), 975 (1994).
- [4] Stedman G. E., Rep. Prog. Phys. **60**,615 (1997).
- [5] Stedman G. E., Schreiber K. U., Bilger H. R., Class. Quant. Grav. **20**, 2527 (2003)
- [6] Schreiber K. U., Velikoseltsev A., Rothacher M., Klügel T., Stedman G. E., Wiltshire D.L., Journal of Geophys. Res. **B109**, B06405 (2004).
- [7] Ashtekar A., Magnon A., J. Math. Phys. **16**, 341 (1975).

- [8] Anderson J. L., Ryon J.W., Phys. Rev. **181**, 1765 (1969).
- [9] Ryon J. W., Anderson J. L., Phys. Rev. D **2**, 2745, (1970).
- [10] Berry M. V., Proc. R. Soc. London **A392**, 46 (1984)
- [11] Kugler M., Shtrikman S., Phys. Rev. **D37**, 934 (1988).
- [12] Benn I. M., Tucker R.W., Phys. Rev **D39**, 1594 (1989).
- [13] Neutz R., Phys. Rev. A **51**, 5039 (1995)
- [14] Benn, I. M. and Tucker, R. W. *An Introduction to Spinors and Geometry with Applications in Physics*. Adam Hilger, IOP Publishing (1987).
- [15] D Burton, A Noble, R W Tucker, Wiltshire D.L., in preparation.
- [16] Page D. N., Class. Quant. Grav. **15**, 1669 (1998)
- [17] Abraham R., Marsden J. E., Ratiu T. *Manifolds, Tensor Analysis and Applications.*, 2nd ed., Springer (1988).